Analyst

Accepted Manuscript

ROYAL SOCIETY OF CHEMISTRY

www.rsc.org/analyst

A WS_2 nanosheet-based platform for fluorescent DNA detection via PNA-DNA hybridization

Shuting Wang, Yulin Zhang, Yong Ning*, Guo-Jun Zhang*

School of Laboratory Medicine, Hubei University of Chinese Medicine, 1 Huangjia Lake West Road, Wuhan 430065, China

*Corresponding author: Tel: +86-27-68890259, Fax: +86-27-68890071

E-mail: zhanggj@hbtcm.edu.cn; ningyong128@163.com

Abstract

WS_2 nanosheet, one of two-dimensional layered nanomaterials, shows high fluorescence quenching ability to the dye-labeled ssDNA. Currently, most of the fluorescent DNA detections employ DNA as a probe for recognition of target DNA. Peptide nucleic acid (PNA) is a DNA mimic but a neutral molecule, showing superior hybridization properties to target DNA. Based on the unique properties of WS_2 nanosheet and PNA-DNA hybridization, we have developed a rapid, simple, stable and sensitive approach for DNA detection based on good fluorescence quenching ability of WS_2 nanosheet as well as high binding affinity and specificity of PNA to DNA. This novel assay is capable of exhibiting high sensitivity and specificity with a detection limit of 500 pM, and discriminating single-base difference.

1. Introduction

DNA plays an important role in life science. DNA detection is critical in the fields of disease diagnosis, forensic investigation, genomics, and etc. Real-time quantification polymerase chain reaction (qPCR), a main approach for DNA detection currently, excels in both amplification and quantification of target sequences, possessing high sensitivity and specificity, as well as capability for SNP genotyping.[1] However, it also has some disadvantages, such as time-consuming, complex, expensive and so on.[2] Thus, it is very necessary to develop rapid, simple and cost-effective DNA assays.

Nanomaterials like nanoparticles,[3-6] quantum dots (QDs),[7, 8] carbon nanotubes (CNTs),[9-11] silicon nanowire (SiNW),[12-14] nanobelts[15, 16], nanospheres[17] and graphene oxide (GO)[18-20] have been widely applied for rapid and sensitive DNA detection due to their special properties. Based on these materials, a series of methods have been developed, including colorimetric assays,[4, 21, 22] fluorescent assays,[7, 10, 18] turbidity assays[23] and electrical assays[9, 12, 24, 25]. In particular, fluorescent assays that using nanomaterials as quenchers have been extensively explored for their simple, rapid and cost-effective merits. As a typical example, single chain fluorescence-labeled DNA probe can be bound to the nanomaterials and fluorescence quench subsequently occurs in the absence of target. However, it releases from the nanomaterials and fluorescence recovers when mixing with complementary target and forming duplex[19]. GO, a two-dimensional material that derives from graphene, is a widely used nanoquencher for this kind of assay owing to its capability of long-range

energy transfer.[18, 19, 26] as well as distinguished adsorption to single stranded (ss-) and double stranded (ds-) DNA. It has got intensive research by using various probes (e.g., DNA,[18, 19] RNA,[27] aptamer,[18, 19] PNA,[20, 28] LNA,[29] MB,[30, 31] etc.) and strategies (e.g., pre-mixing[18] and post-mixing[19], direct detection[18, 19] and amplified detection[32, 33], etc.) to meet the desired sensing performace. Recently, some other two-dimensional layered nanomaterials have been explored as nanoquenchers as well. For example, MoS_2,[34] carbon nitride[35] and WS_2[36] nanosheets were reported to be used in novel fluorescent DNA assays already. WS_2 nanosheet, with a "S-W-S" sandwich structure[37, 38] layer, is reported to have similar effect with GO on the fluorophore labeled DNA probes.[36, 39-41] Compared to GO, the WS_2 preparation doesn't involve oxide treatment while it is a critical process in the GO preparation. As known, the oxidization degree of GO has significant impact on fluorescence quenching efficiency,[42, 43] meaning that the performance of WS_2 nanosheet is more controllable than that of GO. Thus WS_2 is showing great potentials in biosensors.

PNA is a DNA mimic consisting of normal DNA bases and a "peptide-like" backbone.[44] It can hybridize with the complementary nucleic acid sequence obeying the Watson Crick hydrogen-bonding rules and form duplex like DNA does.[45] Moreover, the replacement of negatively-charged sugar-phosphate in DNA by neutral N-(2-aminoethyl)glycine units in PNA[44] affords PNA many advantages over DNA. For instance, the binding affinity and the sequence specificity of PNA probe to nucleic acid target are higher than that of DNA probe.[46, 47] In addition, the PNA-DNA duplex is more stable than the DNA-DNA duplex.[47] Due to these advantages, PNA has been

used in various biosensors[20, 47-51] to improve the sensing performance. For example, in fluorescence assays, GO / PNA sensing systems have proven to be more sensitive[20] or stable[28] than GO / DNA sensing systems. However, PNA has not been explored as probe yet in the WS_2-based platform. In this work, we report a new WS_2 platform based fluorescent DNA assay by using the more specific PNA probe instead of the DNA probe. We investigate the interactions between PNA and WS_2 nanosheet, and develop the DNA sensing platform by PNA and WS_2 based homogeneous fluorescence assay and a post-mixing strategy.

2. Experimental Section

2.1 Materials and Apparatus

The PNA probe sequence used in this work was synthesized by Bio-synthesis, Inc. (Lewisville, Texas), and the DNA sequences were synthesized and purified by Takara biotechnology Co., Ltd. (Dalian, China). Their sequences are as follow:

PNA probe (P1): N-AACCACACAACCTACTACCTCA-lysine-FAM-C

DNA probe (P2): 5'-AACCACACAACCTACTACCTCA-FAM-3'

The complementary target DNA (T1): 5'-TGAGGTAGTAGGTTGTGTGGTT-3'

The one-base mismatched ssDNA (T2): 5'-TGAGGTAGTAGGATGTGTGGTT-3'

The non-complementary ssDNA (T3): 5'-ATGCATGCATGCATGCATGCAA-3'

Tungsten Disulfide (WS_2) nanosheet was purchased from Nanjing XF Nano Material Tech Co., Ltd. (Nanjing, China). Other reagents were of analytical grade.

Ultrapure water was obtained from Millipore water purification system. The fluorescence measurements were taken on a Hitachi F-4600 spectrophotometer.

2.2 Fluorescence assays

In optimizing the concentration of WS_2 nanosheet, the fluorescent probe P1 or P2 (1 μM, 20 μl) was added into a certain amount of 20 mM Tris-HCl buffer (150 mM NaCl, pH=7.6), and then mixed with different amount of WS_2 nanosheet, making the final volume of 1 ml. The mixture was incubated at room temperature for 1 min before fluorescence measurement.

In the kinetic study of WS_2 quenching behavior to the fluorescent probe P1, fluorescence emission spectra were monitored as a function of time after P1 (20 nM) was mixed with WS_2 nanosheet (4 μg/ml).

In the concentration gradient assay, P1 (20 nM) was hybridized with the different concentrations of complementary target T1 (1 nM, 2 nM, 5 nM, 10 nM, 20 nM, 40 nM and 80 nM) at room temperature for 10 min. Then the reaction solution was mixed with WS_2 nanosheet (4 μg/ml) and the mixture was incubated for 1 min before fluorescence measurement.

In the specific DNA detection assay, P1 (20 nM) was hybridized with the target T1, the one-base mismatched ssDNA T2 or the non-complementary T3 of 20 nM at room temperature for 10 min. After that, the reaction solution was mixed with WS_2 nanosheet (4 μg/ml) and the mixture was incubated at the temperature at 65 °C for 1.5 h before fluorescence measurement.

3. Results and Discussion

3.1 Design of the sensing strategy

It has been reported that PNA and DNA have different adsorption behavior at electrically charged surfaces.[52, 53] Consistent with this, previous studies show that PNA has stronger binding affinity to the negatively charged GO nanosheet than DNA does, as the dye-labeled PNA needs less GO than the dye-labeled ssDNA to completely quench the fluorescence of the dye.[20, 28] According to the recent reports in which the dye-labeled ssDNA can be adsorbed on WS_2 nanosheet and subsequently WS_2 quenches its fluorescence,[36, 39] we anticipate that the dye-labeled PNA has the similar interaction with WS_2, and it thus can be employed as a more specific probe in WS_2 platform for DNA detection. To investigate the applicability of PNA probe in this platform and develop a new DNA biosensor, we design a homogeneous fluorescence assay by employing WS_2 and PNA with the schematic shown in Fig 1. PNA instead of DNA is chosen as the probe, and PNA is FAM-labeled at the C-terminal. In the absence of the target, PNA is strongly absorbed on the surface of WS_2, and the fluorescence of FAM can be effectively quenched by WS_2. In contrast, in the presence of the target, PNA-DNA duplex will form immediately and the molecular conformations alter, resulting in weak interaction between the duplex and WS_2, and thus the fluorescence of FAM largely remains.

The WS_2 nanosheets were characterized by both transmission electron microscopy (TEM, JEM-2100) and atomic force microscopy (AFM, Vecco 3D). The TEM image (Fig. S1) revealed that the WS_2 was a two-dimentional thin nanosheet.

AFM images (Fig. S2) further confirmed that the height of the WS_2 sheet was about 1.0 nm, indicating the WS_2 is a single-layer nanosheet.

Fig. 2 confirms the feasibility of the designed assay. P1 (20 nM) in Tris-HCl buffer showed strong fluorescence emission around the wavelength of 520 nm for the labeled FAM fluorophore. With the addition of WS_2, up to 97% quenching of the fluorescence emission was observed. The phenomena indicate strong adsorption of P1 on WS_2 and high fluorescence quenching efficiency of WS_2. However, when P1 was hybridized with the complementary target DNA T1 to form a duplex, its fluorescence was largely retained in the presence of WS_2. It suggests that the adsorption of PNA-DNA duplex on WS_2 is very weak. We speculate that the interactions are induced by the van der Waals force[34] and the hydrophobic force between the nucleobases of PNA and the basal plane of WS_2 as the surface of the WS_2 nanosheet is made of chemically saturated sulfur atoms and is therefore hydrophobic.[54] After P1 is hybridized with T1, the nucleobases are buried into duplex, resulting in the weak interaction between the duplex and WS_2. The fluorophore-labeled P1 is away from the surface of WS_2, so the fluorescence is remained.

3.2 Optimization of WS_2 concentration

The effect of WS_2 concentration on the fluorescence intensity of P1 was investigated. As shown in Fig. 3a, the concentration of WS_2 intensively influenced the fluorescence intensity of P1. With the increase of WS_2 concentration, the fluorescence decreased and trended to a minimum value at 4 μg/ml. Thus, 4 μg/ml WS_2 was used in the following experiments.

As a comparison, the effect of WS_2 concentration on the fluorescence intensity of DNA probe (P2) was also explored. The intensity decreased with the increase of WS_2 concentration (Fig 3b), but the change was much smaller than that of P1 at every WS_2 concentration. This means that the binding affinity of DNA to WS_2 is not as strong as the affinity of PNA to WS_2. The fluorescence of P2 did not decrease to a minimum at 4 μg/ml WS_2, suggesting that DNA probe needs more WS_2 than PNA to completely quench the fluorescence. Then we could conclude that PNA probe is better than DNA probe in consideration of WS_2 concentration and the background signal.

The different binding affinities of WS_2 to PNA and DNA may ascribe to the electrostatic repulsion. It is well known that PNA is neutral while DNA is negatively charged due to their distinctively different backbone. The single-layer WS_2 can be viewed as a positively charged plane of tungsten atoms sandwiched between two planes of negatively charged sulfur atoms[37]. Recently, Ge et al and Liu et al experimentally demonstrated that there were negative charges on the WS_2 nanosheet surface via the zeta potential detection[40, 41]. Based on these studies, we speculate that the WS_2 nanosheet in this work also has negative charges on the surface. If the neutral PNA mixes with WS_2 in Tris-HCl buffer, there would be no repulsion and PNA adsorbs on WS_2 due to the van der Waals force and the hydrophobic force. Thus the binding affinity is extremely strong. However, when DNA mixes with WS_2 in the same condition, both the electrostatic repulsion and the adsorption induced by the two

force mentioned above would exist, resulting in poor binding affinity between DNA and WS_2.

3.3 Kinetic behavior of PNA and WS_2

The kinetic behavior of PNA and WS_2 was studied by monitoring the fluorescence intensity as a function of time. Fig. 4 shows the fluorescence quenching of P1 in the presence of WS_2 as a function of incubation time. It was seen that PNA adsorption on WS_2 surface was very fast at room temperature. It reached equilibrium in 1 min. So 1 min was chosen as the detection time after WS_2 was added into solution.

3.4 Detection of DNA with PNA and WS_2

To explore if the detection system can be applied for quantitative DNA assay, the fluorescence responses induced by T1 at different concentrations were monitored. As shown in Fig. 5a, the fluorescence intensity was gradually enhanced with the increase of target concentrations. This is because T1 hybridizes with P1 and forms PNA-DNA duplex, and the fluorescence of FAM in duplex retains after mixing with WS_2. At the same time, the fluorescence of un-hybridized P1 is efficiently quenched by WS_2 if T1 is less than P1.

Fig. 4b shows the plot of $(F-F_0)$ (the fluorescence intensity at 520 nm) versus the concentration of T1. There is a linear range between 1 and 20 nM with the linear equation $y = 9.67x - 4.38$, and the correlation coefficient is $r = 0.9986$. The limit of detection (LOD) for DNA is 500 pM, which is comparable to the previously reported GO and MoS_2-based DNA sensing systems[19, 20, 34]. Compared with the poly(acridic

acid)-modified WS_2 nanosheet system[36], the LOD in this assay is one order of magnitude higher than that. This is possibly because of WS_2 size dependence, as discussed in the size-dependent GO sensors for ions detection[55]. However, the dosage of WS_2 and the analysis time in this assay is much less than those in that system.

3.5 The specificity of the sensing system

To confirm the sequence specificity of the sensing system, a comparison of the fluorescence signal induced by the target-DNA (T1), the one-base mismatched DNA (T2) and the non-complementary DNA (T3) was performed. The thermal stability of PNA-DNA duplex is strongly affected by the presence of imperfect matches.[47] According to the report, a single base mismatch leads to 8-20 °C decrease in Tm.[45] And the Tm for the complementary PNA-DNA duplex in our experiment was predicted to be 70.5 °C.[13, 56] Then we chose 65 °C as the experiment condition, a temperature lower than 70.5 °C, but higher than the Tm of P1-T2 duplex. We expect that at this temperature a large amount of P1-T1 would maintain the structure of duplex and keep away from WS_2 to retain the fluorescence, while most of P1-T2 duplex would uncoiling and the free P1 adsorbs on WS_2 to quench the fluorescence. The reason is that the adsorption between P1 and WS_2 is rather strong and it would compete with the re-hybridization of target and P1. To guarantee that the denaturation reaction would reach equilibrium, the detection was taken after the mixture was incubated for 1.5 h. To get a control, the solution with only P1 (20 nM) and WS_2 (4 μg/ml) was treated under the same condition. Fig. 6 exhibits the comparison of relative fluorescence signal (F/F_0) regarding the three target sequences. The signal for

T1 was about 3 times as much as that for T2 and T3. Moreover, it was found that the signal for T2 was larger than that for T3, which means that the sensor can be used for detection of single-base mutation. This result clearly demonstrates that our DNA assay is of sufficient selectivity to distinguish the complementary DNA from one-base mismatched DNA sequence as well as the non-complementary sequence.

4 Conclusion

In summary, we have demonstrated that WS_2 has strong binding affinity toward PNA as well as high fluorescence quenching ability to the fluorophore-labeled PNA sequence. In contrast, the affinity between WS_2 and PNA-DNA duplex is very weak, which keeps the fluorophore on duplex far from WS_2 surface, resulting in poor fluorescence quench efficiency. Comparing the fluorescence intensities of FAM-PNA with FAM-DNA under the same concentration of WS_2, it is found that FAM-PNA shows lower signal background, meaning that PNA is more suitable as a probe than DNA. Based on WS_2 nanosheet and PNA-DNA hybridization, the homogeneous fluorescence DNA sensor has been successfully developed and possesses good performance. It can quantitatively detect DNA in a linear range from 1 to 20 nM with the detection limit of 500 pM. It shows high specificity to target sequence because the thermal stabilities of PNA-DNA are obviously different between perfect and imperfect duplexes. The mix-and-detect assay can be finished in several minutes because of the quick formation of PNA-DNA duplex and the fast PNA adsorption to WS_2 surface. Moreover, the assay is conducted in a homogeneous solution and

doesn't require separation, making it easy to perform for automation. This work offers another manner for DNA detection in WS_2-based homogeneous fluorescence assay by employing PNA instead of DNA as the probe. The applications of the sensor in real complex samples are under way by minimizing the interference.

Acknowledgment

The authors acknowledge the financial support from the National Natural Science Foundation of China (Nos. 21275040 and 21475034) and the Research Plan Projects of Hubei Provincial Department of Education (No. D20121606).

Notes and references

1. D. Klein, *Trends in molecular medicine*, 2002, **8**, 257-260.
2. C. S. Thaxton, D. G. Georganopoulou and C. A. Mirkin, *Clinica chimica acta; international journal of clinical chemistry*, 2006, **363**, 120-126.
3. L. M. Zanoli, R. D'Agata and G. Spoto, *Anal Bioanal Chem*, 2012, **402**, 1759-1771.
4. R. Elghanian, *Science*, 1997, **277**, 1078-1081.
5. Y. Zhang, L. Wang, J. Tian, H. Li, Y. Luo and X. Sun, *Langmuir : the ACS journal of surfaces and colloids*, 2011, **27**, 2170-2175.
6. H. Li, Y. Zhang, L. Wang, J. Tian and X. Sun, *Chem. Commun.*, 2010, **47**, 961-963.
7. C.-Y. Zhang, H.-C. Yeh, M. T. Kuroki and T.-H. Wang, *Nature Materials*, 2005, **4**, 826-831.
8. W. Lu, X. Qin, Y. Luo, G. Chang and X. Sun, *Microchimica Acta*, 2011, **175**, 355-359.
9. J. Li, H. T. Ng, A. Cassell, W. Fan, H. Chen, Q. Ye, J. Koehne, J. Han and M. Meyyappan, *Nano letters*, 2003, **3**, 597-602.
10. R. Yang, J. Jin, Y. Chen, N. Shao, H. Kang, Z. Xiao, Z. Tang, Y. Wu, Z. Zhu and W. Tan, *Journal of the American Chemical Society*, 2008, **130**, 8351-8358.
11. H. Li, J. Tian, L. Wang, Y. Zhang and X. Sun, *J. Mater. Chem.*, 2010, **21**, 824-828.
12. J.-i. Hahm and C. M. Lieber, *Nano Letters*, 2004, **4**, 51-54.
13. G.-J. Zhang, G. Zhang, J. H. Chua, R.-E. Chee, E. H. Wong, A. Agarwal, K. D. Buddharaju, N. Singh, Z. Gao and N. Balasubramanian, *Nano letters*, 2008, **8**, 1066-1070.
14. G.-J. Zhang and Y. Ning, *Analytica chimica acta*, 2012, **749**, 1-15.
15. X. Sun, Z. Xing, R. Ning, A. M. Asiri and A. Y. Obaid, *Analyst*, 2014, **139**, 2318-2321.

16. H. Li, Y. Luo and X. Sun, *Biosensors and Bioelectronics*, 2011, **27**, 167-171.
17. H. Li, Y. Zhang, T. Wu, S. Liu, L. Wang and X. Sun, *Journal of Materials Chemistry*, 2011, **21**, 4663-4668.
18. C. H. Lu, H. H. Yang, C. L. Zhu, X. Chen and G. N. Chen, *Angewandte Chemie*, 2009, **121**, 4879-4881.
19. S. He, B. Song, D. Li, C. Zhu, W. Qi, Y. Wen, L. Wang, S. Song, H. Fang and C. Fan, *Advanced Functional Materials*, 2010, **20**, 453-459.
20. S. Guo, D. Du, L. Tang, Y. Ning, Q. Yao and G.-J. Zhang, *Analyst*, 2013, **138**, 3216-3220.
21. Y. Guo, L. Deng, J. Li, S. Guo, E. Wang and S. Dong, *ACS nano*, 2011, **5**, 1282-1290.
22. W. Xu, X. Xue, T. Li, H. Zeng and X. Liu, *Angewandte Chemie International Edition*, 2009, **48**, 6849-6852.
23. T. Kang, H. Choi, S.-W. Joo, S. Y. Lee, K.-A. Yoon and K. Lee, *The Journal of Physical Chemistry B*, 2014.
24. J. Wang, *Analytica Chimica Acta*, 2003, **500**, 247-257.
25. F. Wei, P. B. Lillehoj and C.-M. Ho, *Pediatric research*, 2010, **67**, 458-468.
26. P. J. J. Huang and J. Liu, *Small*, 2012, **8**, 977-983.
27. L. Cui, Z. Chen, Z. Zhu, X. Lin, X. Chen and C. J. Yang, *Analytical chemistry*, 2013, **85**, 2269-2275.
28. S.-R. Ryoo, J. Lee, J. Yeo, H.-K. Na, Y.-K. Kim, H. Jang, J. H. Lee, S. W. Han, Y. Lee and V. N. Kim, *ACS nano*, 2013, **7**, 5882-5891.
29. M. Rana, M. Balcioglu, N. Robertson and M. V. Yigit, *Analyst*, 2014, **139**, 714-720.
30. F. Li, Y. Huang, Q. Yang, Z. Zhong, D. Li, L. Wang, S. Song and C. Fan, *Nanoscale*, 2010, **2**, 1021-1026.
31. J.-J. Liu, X.-R. Song, Y.-W. Wang, G.-N. Chen and H.-H. Yang, *Nanoscale*, 2012, **4**, 3655-3659.
32. L. Peng, Z. Zhu, Y. Chen, D. Han and W. Tan, *Biosensors & bioelectronics*, 2012, **35**, 475-478.
33. X. J. Xing, X. G. Liu, Y. He, Y. Lin, C. L. Zhang, H. W. Tang and D. W. Pang, *Biomacromolecules*, 2013, **14**, 117-123.
34. C. Zhu, Z. Zeng, H. Li, F. Li, C. Fan and H. Zhang, *J Am Chem Soc*, 2013, **135**, 5998-6001.
35. Q. Wang, W. Wang, J. Lei, N. Xu, F. Gao and H. Ju, *Anal Chem*, 2013, **85**, 12182-12188.
36. Y. Yuan, R. Li and Z. Liu, *Anal Chem*, 2014, **86**, 3610-3615.
37. C. Ataca, H. Sahin and S. Ciraci, *The Journal of Physical Chemistry C*, 2012, **116**, 8983-8999.
38. A. Klein, S. Tiefenbacher, V. Eyert, C. Pettenkofer and W. Jaegermann, *Physical Review B*, 2001, **64**.
39. Q. Xi, D. M. Zhou, Y. Y. Kan, J. Ge, Z. K. Wu, R. Q. Yu and J. H. Jiang, *Anal Chem*, 2014, **86**, 1361-1365.
40. J. Ge, L.-J. Tang, Q. Xi, X.-P. Li, R.-Q. Yu, J.-H. Jiang and X. Chu, *Nanoscale*, 2014, **6**, 6866-6872.
41. J. Ge, X. Wang, Z. Wu, G. Shen and R. Yu, *Analytical Methods*, 2014.
42. L. Zeng, Y. Yuan, P. Shen, K. Y. Wong and Z. Liu, *Chemistry-A European Journal*, 2013, **19**, 8063-8067.
43. Z. Li, M. He, D. Xu and Z. Liu, *Journal of Photochemistry and Photobiology C: Photochemistry Reviews*, 2014, **18**, 1-17.

44. P. E. Nielsen, M. Egholm and O. Buchardt, *Bioconjugate chemistry*, 1994, **5**, 3-7.
45. M. Egholm, O. Buchardt, L. Christensen, C. Behrens, S. M. Freier, D. A. Driver, R. H. Berg, S. K. Kim, B. Norden and P. E. Nielsen, 1993.
46. P. E. Nielsen and M. Egholm, *Curr. Issues Mol. Biol*, 1999, **1**, 89-104.
47. J. Wang, *Biosensors and Bioelectronics*, 1998, **13**, 757-762.
48. V. V. Demidov, 2013.
49. G.-J. Zhang, J. H. Chua, R.-E. Chee, A. Agarwal, S. M. Wong, K. D. Buddharaju and N. Balasubramanian, *Biosensors and Bioelectronics*, 2008, **23**, 1701-1707.
50. X. Luo and I. M. Hsing, *Electroanalysis*, 2009, **21**, 1557-1561.
51. E. Socher, L. Bethge, A. Knoll, N. Jungnick, A. Herrmann and O. Seitz, *Angewandte Chemie International Edition*, 2008, **47**, 9555-9559.
52. M. Fojta, V. Vetterl, M. Tomschik, F. Jelen, P. Nielsen, J. Wang and E. Palecek, *Biophysical journal*, 1997, **72**, 2285-2293.
53. J. Wang, G. Rivas, X. Cai, M. Chicharro, N. Dontha, D. Luo, E. Palecek and P. E. Nielsen, *Electroanalysis*, 1997, **9**, 120-124.
54. F. Kopnov, A. Yoffe, G. Leitus and R. Tenne, *physica status solidi (b)*, 2006, **243**, 1229-1240.
55. H. Zhang, S. Jia, M. Lv, J. Shi, X. Zuo, S. Su, L. Wang, W. Huang, C. Fan and Q. Huang, *Analytical chemistry*, 2014, **86**, 4047-4051.
56. U. Giesen, W. Kleider, C. Berding, A. Geiger, H. Ørum and P. E. Nielsen, *Nucleic acids research*, 1998, **26**, 5004-5006.

Figure captions:

Fig. 1 Scheme of WS_2 nanosheet platform for fluorescent DNA detection by employing PNA as a probe.

Fig. 2 Fluorescence emission spectra of PNA probe in Tris-HCl buffer, PNA probe mixed with WS_2, and PNA-DNA duplex mixed with WS_2, respectively. The concentration of PNA probe and PNA-DNA duplex were 20 nM while the WS_2 concentration was 4 μg/ml. Excitation: 495 nm, emission: 520 nm.

Fig. 3 Fluorescence quenching of (a) PNA probe and (b) DNA probe without and with various concentrations of WS_2 nanosheet (1, 2, 3, 4, and 5 μg/ml).

Fig. 4 Fluorescence quenching of PNA probe (20 nM) in Tris-HCl buffer by WS_2 nanosheet (4 μg/ml) as a function of time.

Fig. 5 (a) Fluorescence spectra of PNA probe (20 nM) in the presence of different concentrations of cDNA (1, 2, 5, 10, 20, 40, 80 nM). (b) The dependence of the fluorescence intensity change (F-F0) on cDNA concentration and the linear calibration within the range of 1-20 nM. F and F_0 are fluorescence intensities with and without cDNA, respectively. The data shown in the figures represent the average of three independent experiments.

Fig. 6 The specificity of the fluorescent DNA assay. The bars represent the relative fluorescence intensity upon addition of 20 nM of cDNA, one-base mismatched DNA and non-complementary DNA, respectively.

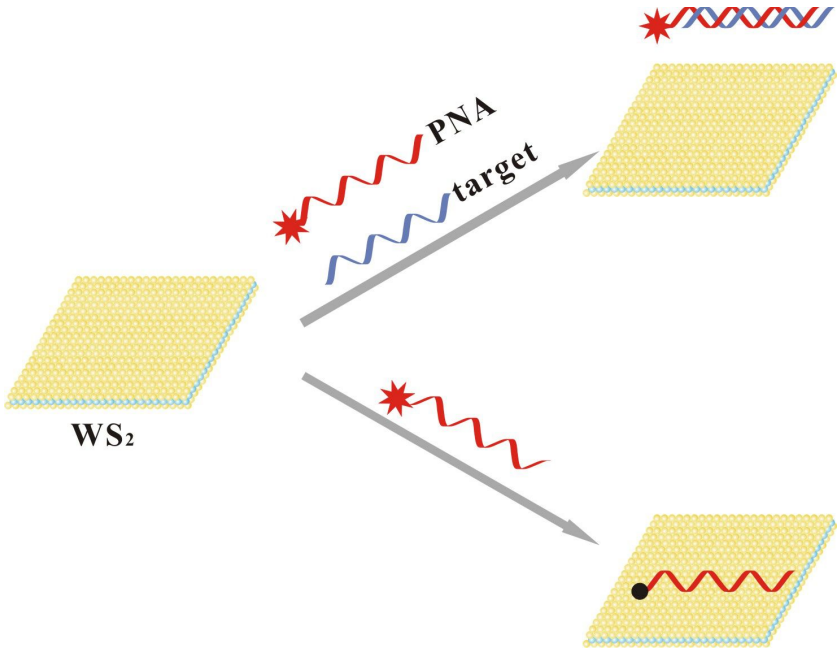

Figure 1

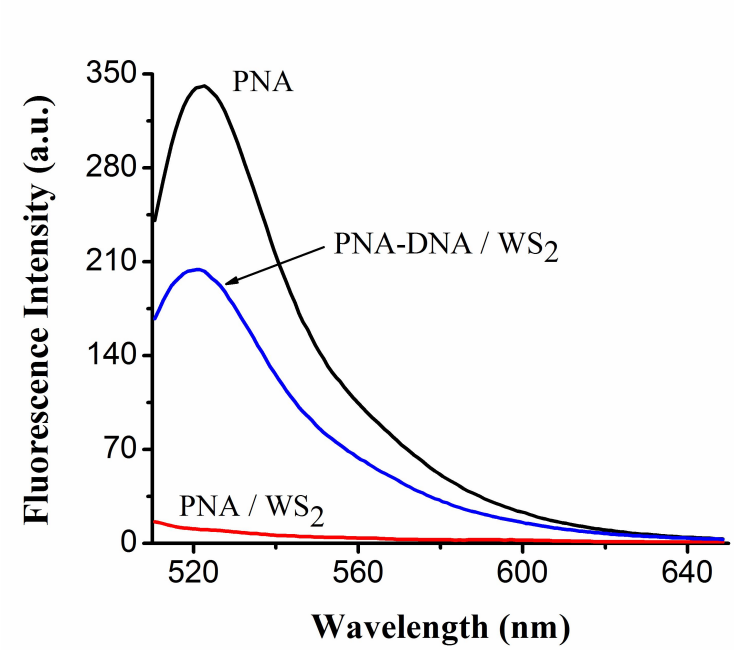

Figure 2

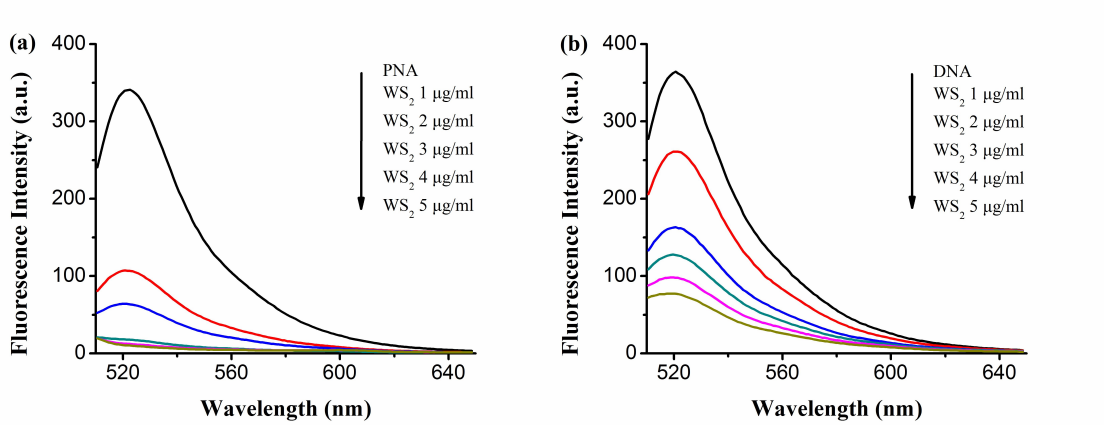

Figure 3

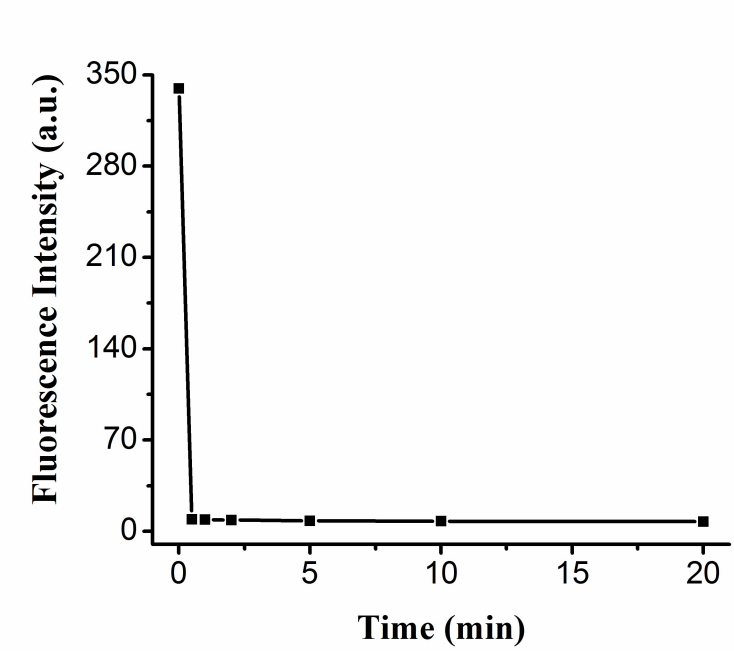

Figure 4

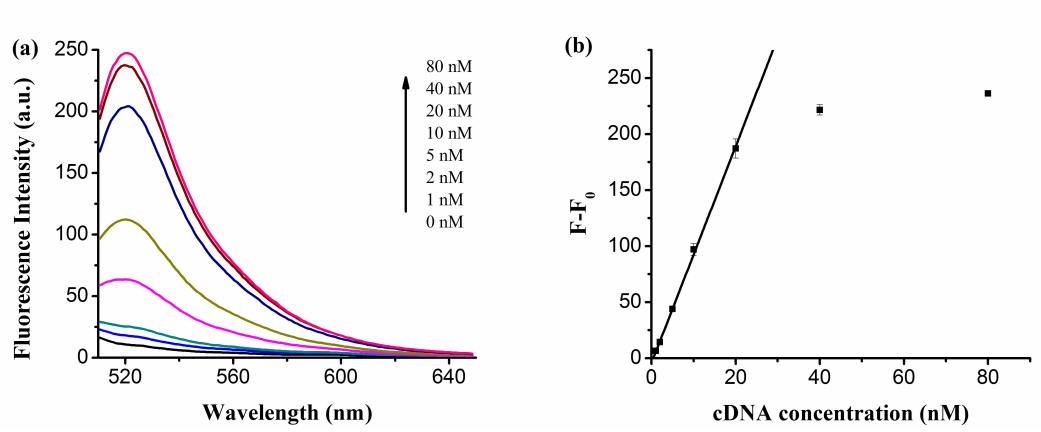

Figure 5

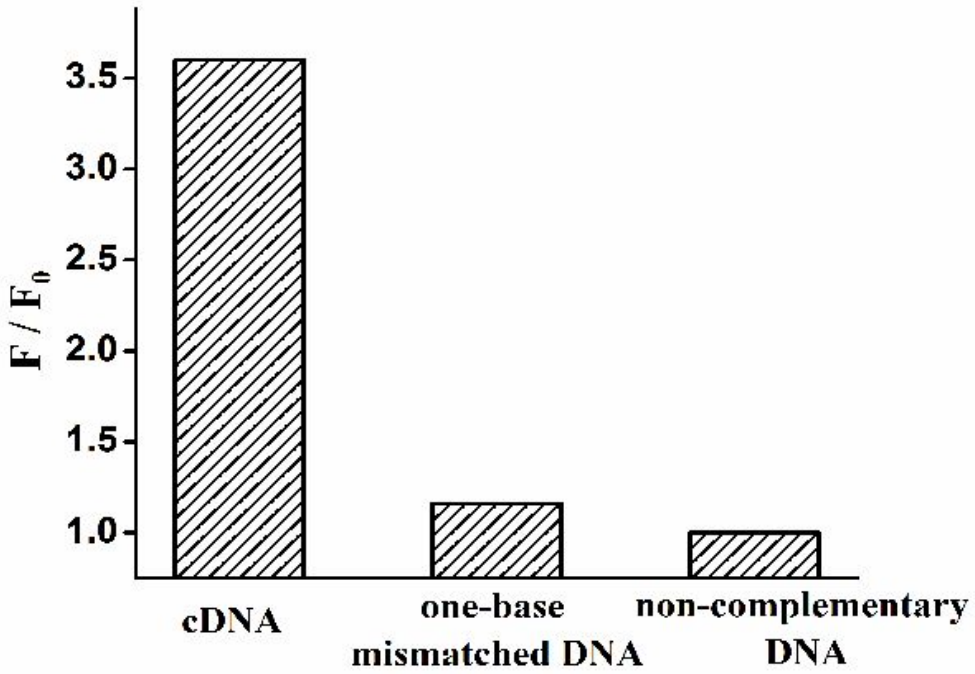

Figure 6